




Clinical and Preclinical Evidence for M₁ Muscarinic Acetylcholine Receptor Potentiation as a Therapeutic Approach for Rett Syndrome

Mackenzie Smith^{1,2} · Bright Arthur^{3,4,5} · Jakub Cikowski^{1,2} · Calista Holt^{1,2} · Sonia Gonzalez^{1,2} · Nicole M. Fisher^{3,4,5} · Sheryl Anne D. Vermudez^{3,4,5} · Craig W. Lindsley^{3,4,5,6,7} · Colleen M. Niswender^{3,4,5,6,8} · Rocco G. Gogliotti^{1,2,3,4} 

Accepted: 24 May 2022 / Published online: 7 June 2022
© The Author(s) 2022

Summary

Rett syndrome (RTT) is a neurodevelopmental disorder that is characterized by developmental regression, loss of communicative ability, stereotyped hand wringing, cognitive impairment, and central apneas, among many other symptoms. RTT is caused by loss-of-function mutations in a methyl-reader known as methyl-CpG-binding protein 2 (MeCP2), a protein that links epigenetic changes on DNA to larger chromatin structure. Historically, target identification for RTT has relied heavily on *Mecp2* knockout mice; however, we recently adopted the alternative approach of performing transcriptional profiling in autopsy samples from RTT patients. Through this mechanism, we identified muscarinic acetylcholine receptors (mAChRs) as potential therapeutic targets. Here, we characterized a cohort of 40 temporal cortex samples from individuals with RTT and quantified significantly decreased levels of the M₁, M₂, M₃, and M₅ mAChRs subtypes relative to neurotypical controls. Of these four subtypes, M₁ expression demonstrated a linear relationship with *MeCP2* expression, such that M₁ levels were only diminished in contexts where MeCP2 was also significantly decreased. Further, we show that M₁ potentiation with the positive allosteric modulator (PAM) VU0453595 (VU595) rescued social preference, spatial memory, and associative memory deficits, as well as decreased apneas in *Mecp2*^{+/-} mice. VU595's efficacy on apneas in *Mecp2*^{+/-} mice was mediated by the facilitation of the transition from inspiration to expiration. Molecular analysis correlated rescue with normalized global gene expression patterns in the brainstem and hippocampus, as well as increased Gsk3β inhibition and NMDA receptor trafficking. Together, these data suggest that M₁ PAMs could represent a new class of RTT therapeutics.

Keywords Rett syndrome · Brainstem · Apneas · Cognition · M₁ mAChR · Gsk3β

Introduction

Loss-of-function mutations in the *Methyl-CpG-Binding Protein 2 (MeCP2)* gene are linked to a neurodevelopment disorder known as Rett syndrome (RTT) [1]. MeCP2 is a methyl reader protein that epigenetically regulates gene transcription either positively or negatively, depending upon its binding partners [2]. Pathogenic mutations in MeCP2 primarily either destabilize the protein, disrupt its ability to bind methylated DNA, or prevent its association with the nuclear receptor corepressor (NCoR) complex [3, 4]. RTT patients exhibit a myriad of symptoms that include developmental regression, loss of communicative ability, impaired social engagement, compulsive hand wringing, and respiratory dysfunction [5, 6].

Similar to other neurological disorders, RTT therapeutic targets are traditionally identified through expression or functional analysis in *Mecp2* knockout mice. Motivated by

✉ Rocco G. Gogliotti
rgogliotti@luc.edu

¹ Department of Molecular Pharmacology and Neuroscience, Loyola University Chicago, Maywood, IL 60153, USA

² Edward Hines Jr. VA Hospital, Hines, IL 60141, USA

³ Department of Pharmacology, Vanderbilt University, Nashville, TN 37232, USA

⁴ Warren Center for Neuroscience Drug Discovery, Vanderbilt University, Nashville, TN 37232, USA

⁵ Vanderbilt Kennedy Center, Vanderbilt University Medical Center, Nashville, TN 37232, USA

⁶ Vanderbilt Institute of Chemical Biology, Vanderbilt University, Nashville, TN 37232, USA

⁷ Department of Chemistry, Vanderbilt University, Nashville, TN 37232, USA

⁸ Vanderbilt Brain Institute, Vanderbilt University, Nashville, TN 37232, USA

the high failure rate of promising preclinical compounds to translate into effective therapeutics [7], we recently adopted the alternative strategy of performing transcriptional profiling in autopsy samples from RTT patients. Through this mechanism, we sought to identify potential targets that would originate from a position of translational relevance that could be back-modeled in rodents for safety and efficacy studies [8, 9]. Using this approach, we previously identified conserved disruption of mRNA from four of the five subtypes of muscarinic acetylcholine receptors (mAChRs) in nine motor cortex and six cerebellar RTT samples compared relative to age, sex, and postmortem interval matched controls [8]. As a proof of concept, we demonstrated that a positive allosteric modulator (PAM) of the mAChR subtype 4 (M₄) improved cognitive, social, and respiratory symptom domains in *Mecp2*^{+/-} mice.

Decreased cholinergic tone is a well-established aspect of RTT pathophysiology in patients which predates the discovery of *MeCP2* as the causative gene. In RTT autopsy samples, both decreased choline acetyltransferase (ChAT) activity and radiolabeled vesamicol binding have been reported in the putamen and in the thalamus [10, 11]. Similar results are also observed in *Mecp2*^{+/-} rats, where decreased acetylcholine levels are observed at symptomatic ages while all other neurotransmitters remain unaffected [12]. Data from RTT mouse models agree with these findings, as loss of *Mecp2* in cholinergic neurons evokes comparable anxiety, motor, social, cognitive, and cardiac phenotypes to what is observed with global *Mecp2* knockout [13–15]. Notably, these phenotypes also appear to be responsive to compounds that increase cholinergic tone such as donepezil, PNU282987, and dietary choline [13, 14, 16], as well as to viral delivery of *MeCP2* to cholinergic neurons in RTT model mice [15]. These data reinforce the hypothesis that methods of targeting cholinergic neurotransmission may have utility as RTT therapeutics and align with our data in autopsy samples that support the use of compounds that specifically potentiate mAChR signaling.

The clinical development of mAChR modulators has a robust and complex history, highlighted by seminal studies in the 1980s showing efficacy in cognitive and social symptom domains with administration of the M₁-preferring, nonselective agonist xanomeline in patients with Alzheimer's disease (AD) [17, 18]. While hypercholinergic adverse effects plagued mAChR discovery programs, recent advancements have shown promise in clinical trials and provided renewed hope [19]. In this study, we use a series of 40 temporal cortex samples from RTT autopsies to show that decreased M₁ mAChR expression is both highly conserved and exhibits a linear relationship with MeCP2 expression. Further, we demonstrate that administration of the selective M₁ PAM VU0453595 (VU595) normalizes social interaction phenotypes, rescues associative and spatial learning defects, and

decreases apneas in RTT model mice while producing no overt adverse effects. We also show that treatment with VU595 normalizes global gene expression patterns in *Mecp2*^{+/-} animals and rescues pathways associated with Gsk3 β inhibition and NMDA receptor (NMDAR) trafficking. Together, these data support the continued development of M₁ mAChR positive allosteric modulators as potential RTT therapeutics.

Methods

Study Design

Human samples were obtained from the NIH NeuroBioBank and the University of Maryland Brain and Tissue Bank under PHS contract HHSN-271–2013-00,030. The tissues were postmortem and fully de-identified and, as such, are classified as exempt from Human Subject Research regulations. Animal work was conducted under the oversight of the Loyola University and Vanderbilt University Institutional Animal Care and Use Committees.

Mice were assigned to dosing groups at random and phenotyping or molecular quantitation was either performed by a blinded researcher or by automated software. Statistics were carried out using Prism 6.0 (GraphPad) and Excel (Microsoft). All data shown represent mean \pm SEM. Statistical significance between groups was determined using two-tailed unpaired or paired student's *t* tests and one- or two-way analysis of variance (ANOVA), with Bonferroni's or individual student's *t* test post hoc analysis, as specified in each figure legend. Mice sacrificed for gene expression were euthanized using CO₂ inhalation at a flow rate of 2 L per minute, as recommended by the AVMA.

Selection of Animal Model

The selection of mouse model (*Mecp2*^{+/*tm1.1* bird}), sex, and sample size was based on the standards established by the National Institute of Mental Health and RTT research community. Heterozygous female mice were chosen to achieve construct validity, as the overwhelming majority of RTT patients are female and *MeCP2*^{mut/+}. A robust literature also establishes RTT-like phenotypes in this model (face validity), albeit milder than what is observed in humans, and variable in both age of onset and symptom severity, due to random x inactivation [20–22]. To account for variability, we used *N* values of > 10 mice per genotype and treatment group, compared test mice to their own baseline where possible, and performed assays at 20 weeks, when phenotypes become reproducibly observed in virtually all *Mecp2*^{+/-} mice within our colony [8, 9, 23].

RNA-cDNA Preparation

The demographics of autopsy samples used in these studies are summarized in Table S1. Briefly, Brodmann Area (BA) 38 (temporal cortex) samples were received from $N=40$ RTT samples with an age of 22.9 ± 2.1 years and a PMI of 20.2 ± 1.5 h. $N=12$ controls were an age of 21.8 ± 2.4 years and a PMI of 19.3 ± 2.0 h. Approximately 1 g of the temporal cortex was impact-dissociated under dry ice and then pulverized using mortar and pestle under liquid nitrogen. Total RNA and cDNA were prepared from 200 mg of tissue using standard trizol-chloroform methodology. Brain samples from 20-week-old *Mecp2^{+/-}(tm1.1 Bird)* mice were prepared using identical methodology.

mRNA and Protein Analysis

Quantitative real-time (qRT)-PCR was performed on Bio-Rad CFX96 instrumentation using Thermo Fisher Assay on Demand primer-probe kits. The assay IDs used are *CHRM1* (Hs00265195_s1), *CHRM2* (Hs06634238_s1), *CHRM3* (Hs00327458_s1), *CHRM4* (Hs00265219_s1), *CHRM5* (Hs00255278_s1), and *Chrm1* (Mm00432509_s1). Human and mouse samples were normalized to the internal control *G6PD* (Hs00166169_m1; Mm00656735_g1). qRT-PCR data was analyzed using the delta-delta Ct method. Differential RNA-sequencing was performed as previously described [8]. Differentially expressed genes were processed by Reactome.org for pathway enrichment analysis, and false discovery rates were calculated as a function of mapped genes.

Human and mouse protein from 200 mg of tissue was isolated and Western blots were run as previously described [9]. Primary antibodies were used at the following concentrations: Chrm1 (1:1000, Millipore ab5164), Gsk3 α (1:500, CST4337), Gsk3 α S21 (1:500, CST9316), Gsk3 α / β Y216/Y279 (1:500, Fisher 44604G), Gsk3 β (1:500, Abcam ab93926), Gsk3 α S9 (1:500, CST9323), Nmdar2a/b (1:400, Sigma AB1548), Psd-95 (1:1000, CST3450), Gapdh (1:5000, CST5174), and β -Tubulin (1:2000, CST86298). The fluorescent secondary antibodies used were goat anti-mouse 680 (1:5000, LiCor #926-68,070), goat anti-rabbit 680 (1:5000, LiCor #926-68,071), and goat anti-rabbit 800 (1:5000, Li-Cor 926-32211). Images were acquired, and fluorescence was quantified on a Li-Cor Odyssey Infrared Imaging System.

Compound Administration and Phenotyping

In the studies described herein, 20-week-old *Mecp2^{+/-}* and *Mecp2^{+/+}* females were used which represent an age where consistent phenotypes are observed in our colony. Based on the pharmacokinetics and T_{max} of the molecule [24], either vehicle (10% Tween 80) or 10 mg/kg of

VU0453595 (VU595) was administered to *Mecp2^{+/-}* and *Mecp2^{+/+}* female mice (20w) via intraperitoneal (ip) injection 30 min before the start of the phenotypic assay and/or tissue harvest. The order phenotyping was performed was open field, three-chamber social interaction, novel object recognition, whole-body plethysmography, and contextual fear conditioning, with a minimum of 5 days washout between assays.

Behavioral Assays

Open Field

Spontaneous locomotion and anxiety were measured using the open field assay. Test mice were injected with either VU595 or vehicle and placed in the activity monitoring chamber. Exploratory and locomotor behavior was then monitored using Activity software to quantify beam breaks in the X, Y, and Z planes.

3-Chamber Social Preference Assay

Control and test mice were placed in a standard 3-chamber apparatus and allowed to habituate for 7 min. A novel mouse (stranger 1, 6-week-old C57B6, female) that was restrained in a wire cage was then placed in one of the end chambers, and an empty cup was placed in the opposing end chamber. The test mouse was then allowed to explore all 3 chambers for 7 min before being returned to its home cage. After 1 h, the test mouse was returned to the 3-chamber apparatus, and the ability to distinguish between stranger 1 and a novel stranger (stranger 2, 6-week-old C57B6, female) was quantified for 7 min using AnyMaze™ software.

Novel Object Recognition Assay

Novel object recognition (NOR) was conducted as described in [25]. Briefly, test mice were placed inside a chamber with 2 identical objects (a slide box or ball) and allowed to explore for 10 min. The animals were then returned to their home cage. After 1 h, test mice were returned to the chamber a final time for 5 min, and 1 of the 2 objects was replaced with a novel object. The test was video recorded and the seconds spent directly sniffing each object were scored by a blinded reviewer. Discrimination index was defined as $(Time_{novel} - Time_{familiar}) / (Time_{novel} + Time_{familiar})$. Direct sniffing in the novel object recognition assay was defined as an approach where the mouse's nose either made contact or came in close proximity to the object.

Contextual Fear Conditioning

Animals were treated with VU595 and fear-conditioned on day 1 of the task, and the percent of time spent freezing was assessed 24 h later. On the conditioning day, mice were placed into an operant chamber with a shock grid (Med Associates Inc.) in the presence of a 10% vanilla odor cue. Following a 3-min habituation period, mice were exposed to two 1-s 0.7-mA foot shocks spaced 30 s apart. After 24 h, mice were placed back into the same shock chamber with a 10% vanilla odor cue, and the percent of time spent freezing during a 3-min testing period was assessed by Med Associates software.

Whole-Body Plethysmography

Unrestrained *Mecp2*^{+/-} and *Mecp2*^{+/+} mice were placed in a whole-body plethysmograph recording chamber (Buxco, 2-site system) with a continuous inflow of air (1 L/min). Following a habituation period of 30 min, a baseline recording was established for 30 min. Mice were then removed from the chamber, injected with VU595 or vehicle, and re-acclimated for 30 min, and respiratory measurements were made for an additional 30 min. Analysis was performed using FinePointe Research Suite (v2.3.1.9). Apneas, defined as pauses spanning 2× the average expiratory time of the previous 2 min, were quantified using the FinePointe apnea software patch, followed by manual spot-checking of the larger data set. Only periods of motion-free recording were analyzed. All filters were applied while the researchers were blinded to the genotype and treatment group.

Results

M₁ Expression is Decreased in 40 RTT Temporal Cortex Autopsy Samples

Our previous work used RNA-sequencing (RNA-seq) to identify conserved disruption of mAChRs in 9 motor cortex and 6 cerebellar RTT autopsy samples [8]. While among the highest-powered transcriptional profiling studies conducted using RTT autopsy samples, the potential for variability across a larger population must be considered when determining the value of a prospective therapeutic target. To address this, we obtained 40 temporal cortex samples from patients clinically diagnosed with RTT as well as 12 age, sex, and postmortem interval matched controls (Table S1). While fully subtype-selective mAChR antibodies do not exist [26], we isolated protein and compared total (M₁–M₅) mAChR levels via fluorescent Western blot with an M₁-preferring

antibody. These experiments showed a significant decrease in mAChR levels in the temporal cortex of RTT patients relative to matched controls (Fig. 1A–B).

We next performed qRT-PCR to quantify mAChR subtype expression in this larger sample set. As shown in Fig. 1C and Supplemental Fig. 1, we observed a significant reduction in *M₁*, *M₂*, *M₃*, and *M₅* expression. Remarkably, we did not see a significant change in *M₄* expression in the temporal cortex (Fig. 1D), which stands in contrast to what was observed in the motor cortex and cerebellum [8]. To determine whether the expression of any of the mAChR subtypes correlated with *MeCP2* levels, we quantified *MeCP2* mRNA expression and compared it relative to the *M₁*–*M₅* mRNA levels within each patient. These experiments showed a significant linear relationship between *MeCP2* and *M₁* mRNA, such that *M₁* levels are preferentially decreased in a context in which *MeCP2* levels are also decreased (Fig. 1E–F). This relationship was not observed with any of the other mAChRs in RTT patients; however, it was observed with *M₂* and *M₅* expression in controls (Fig. S1). Although limited by the availability of human samples, using the quantified decrease in *M₁* expression, we back-calculated a value of 86.7% power for this analysis (ClinCalc), which exceeds the standard 80% used in many clinical studies.

M₁ Expression is Decreased in the Brainstem of *Mecp2*^{+/-} Mice

When coupled with the recent advancements in M₁ positive allosteric modulator (PAM) drug discovery, the finding that M₁ expression is decreased in the brains of RTT patients is potentially salient. To determine whether this observation also extended to mouse models of RTT, we isolated synaptosomes from the cortex, hippocampus, and brainstem of female 20-week-old *Mecp2*^{+/-} and *Mecp2*^{+/+} mice and performed Western blotting with an M₁-preferring antibody. In contrast to what was observed in human samples, significantly decreased mAChR expression was only observed in the brainstem of *Mecp2*^{+/-} mice (Fig. 1G), potentially indicative of temporal, spatial, and/or species-specific factors contributing to the regulation of M₁ expression.

M₁ Potentiation Rescues Social and Cognitive Deficits in *Mecp2*^{+/-} Mice

Given the significant decrease in M₁ expression in clinical and preclinical sample sets, we next sought to determine whether M₁ potentiation could improve RTT-like phenotypes in *Mecp2*^{+/-} mice. *Mecp2*^{+/-} mice and *Mecp2*^{+/+} littermate controls were treated with either vehicle (10% tween 80) or the M₁-PAM VU595 and progressed through a battery of tests encompassing the major RTT symptom domains, including open field (motor and anxiety),

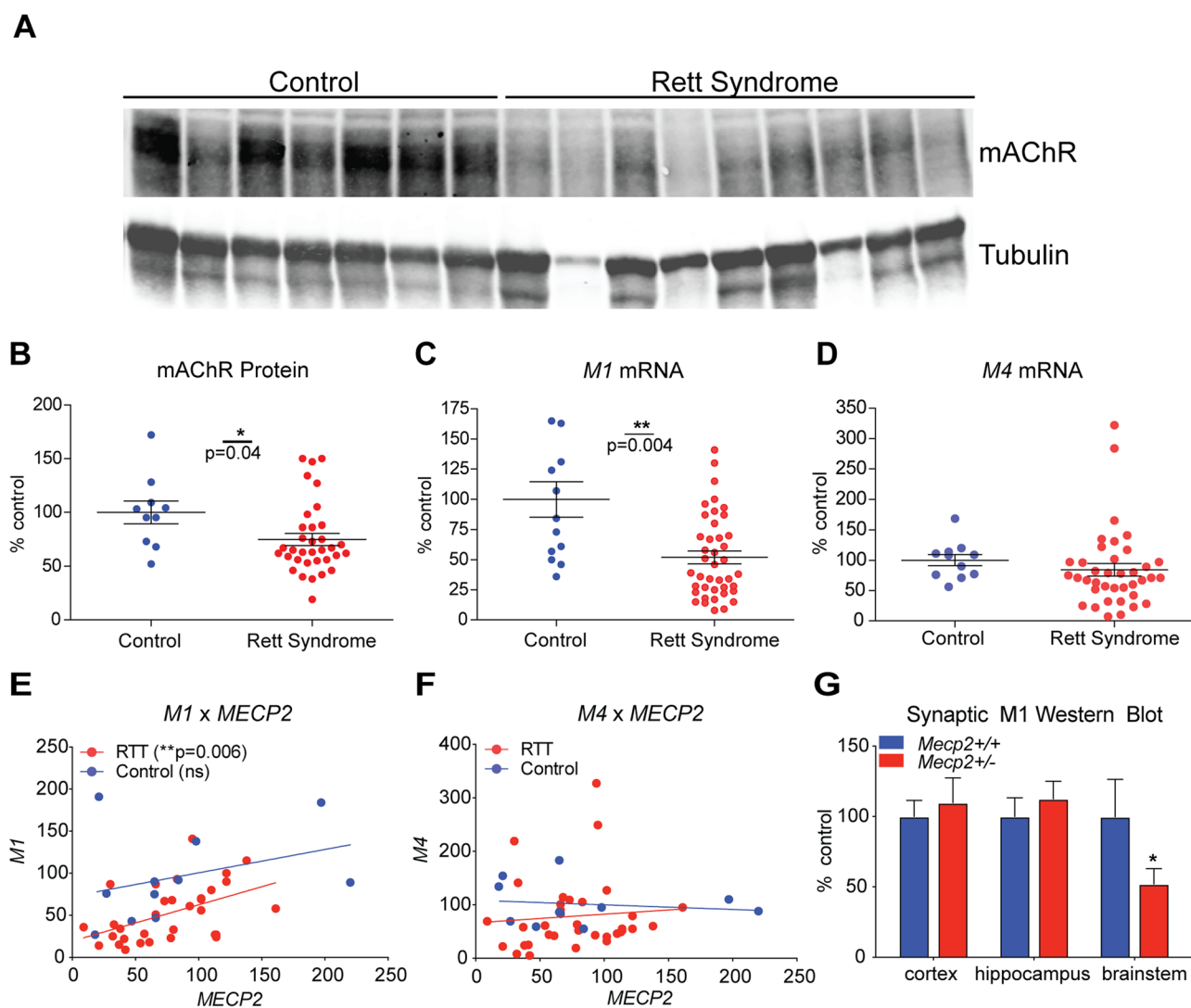


Fig. 1 M_1 expression is decreased in temporal cortex samples from 40 Rett syndrome (RTT) autopsy samples. **A–B** Western blot. mAChR (M_1 – M_5) protein levels are significantly decreased in the brain samples (BA38) from RTT autopsies when compared relative to age, sex, and postmortem interval matched controls ($N=12$). Student's t test. **C–D** qRT-PCR. mRNA expression of the mAChR subtype M_1 receptor is significantly decreased in human RTT samples, while M_4 levels are comparable to controls in the temporal cortex.

Student's t test. **E–F** Linear regression analysis. A correlative analysis shows a significant linear relationship between M_1 and $MeCP2$ transcript levels, which is not observed with M_4 . Linear regression. **G** Western blot. Relative to $Mecp2^{+/+}$ controls, synaptosome preparations from 20-week-old $Mecp2^{+/-}$ mice show a significant reduction in mAChR levels in the brainstem. Two-way ANOVA with Tukey post hoc analysis. $N=5$ /treatment/genotype. * $p < 0.05$, ** $p < 0.01$

three-chamber social interaction (social), novel object recognition (spatial memory), and contextual fear conditioning (associative memory). Mice were treated (ip) 30 min before each test, with a 5-day washout period between assays. The strategy of using a comprehensive phenotypic assessment was chosen to control for the broad expression pattern of the M_1 receptor and the potential for VU595's PAM activity in brain regions with normal expression to either evoke adverse effects, improve phenotypes independent of M_1 expression, and/or influence

interdependent phenotypes (i.e., anxiety and fear conditioning, motor function and sociability).

In the open field assay, we observed no difference in spontaneous locomotion between $Mecp2^{+/-}$ mice and littermate controls, regardless of treatment (Fig. 2A–B). This finding also extended to time spent in the center, where no changes were observed as a function of drug or genotype. In the three-chamber social interaction assay, there was no effect of genotype or drug on the sociability phase of the assay, with all test groups showing a preference for the

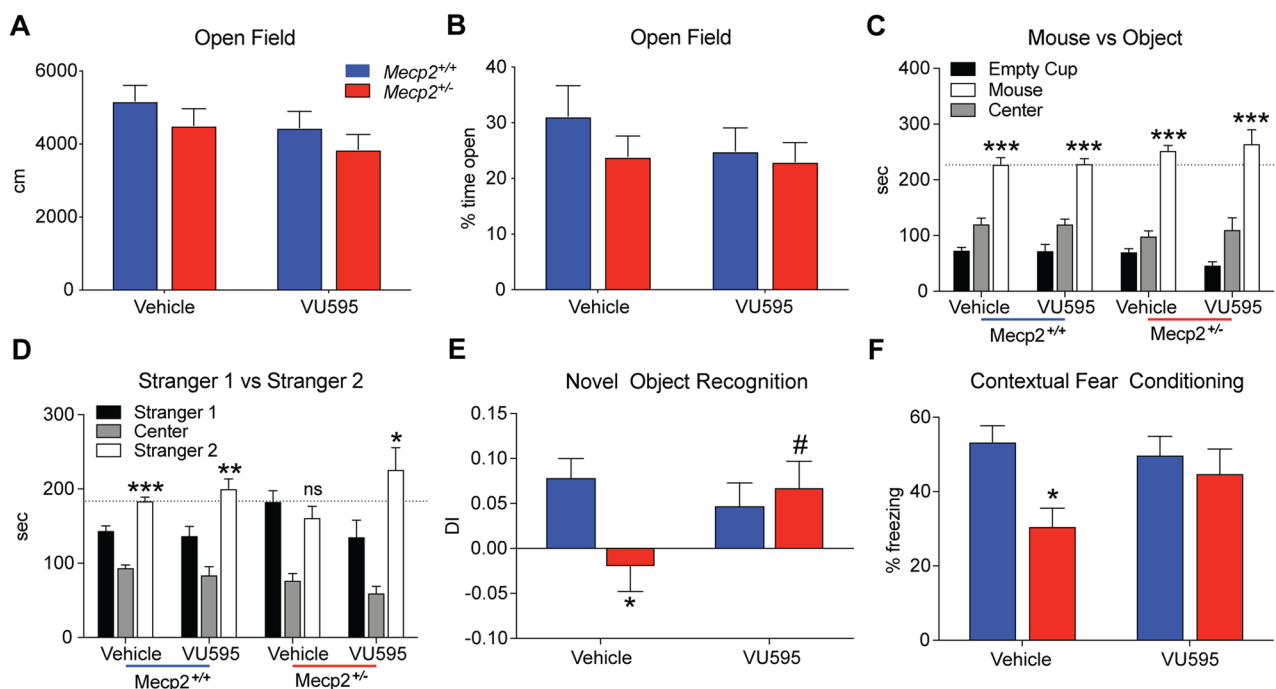


Fig. 2 M₁ potentiation with VU0467595 (VU595) improves social and cognitive phenotypes in the *Mecp2*^{+/-} model of Rett syndrome. *N*=13 *Mecp2*^{+/+}/treatment group, *N*=11 *Mecp2*^{+/-}/treatment group. **A–B** Open field. Neither genotype nor VU595 administration (10 mg/kg, ip) had an impact on spontaneous locomotion (A) and anxiety phenotypes (B) relative to vehicle *Mecp2*^{+/+} control mice. **C–D** Three-chamber social interaction assay. No genotype or compound effect was observed in the sociability phase of the assay (C), as all mice demonstrated a preference for the stranger 1 mouse over the empty cup. When exposed to a familiar (stranger 1) and a novel (stranger 2) mouse, *Mecp2*^{+/+} mice showed a preference for social novelty, independent of treatment. Conversely, vehicle-treated *Mecp2*^{+/-} mice did not distinguish between stranger 1 or stranger 2, and VU595 treatment restored preference for the novel mouse. Two-

way ANOVA with Tukey post hoc analysis. **E** Novel object recognition. DI, discrimination index. Vehicle-treated *Mecp2*^{+/-} mice did not show a preference for the novel object over a familiar object, indicative of a deficit in spatial memory. VU595 administration significantly improved this phenotype in *Mecp2*^{+/-} mice. Two-way ANOVA with Tukey post hoc analysis. **F** Contextual fear conditioning. Vehicle-treated *Mecp2*^{+/-} mice presented with significantly decreased freezing when re-exposed to an aversive environment, suggesting an impairment in associative memory. Treatment with VU595 before the training phase of this assay normalized freezing in *Mecp2*^{+/-} mice to levels comparable to *Mecp2*^{+/+} controls. Two-way ANOVA with Tukey post hoc analysis. Ns, not significant. **p*<0.05, ***p*<0.01, ****p*, 0.001. #*p*<0.05 within genotype comparison

stranger 1 mouse over the empty cup (Fig. 2C). Although not definitive, this finding is important in light of the sensory-perception deficits in RTT model mice [27–31], as it establishes that the capacity of test mice to detect the stranger mouse is comparable to controls. Similar to other studies [8, 9], vehicle-treated *Mecp2*^{+/-} mice failed to show a preference for the novel mouse in the second phase of this assay, while littermate controls spent significantly more time with the stranger 2 mouse, regardless of treatment (Fig. 2D). VU595 treatment significantly improved this parameter in *Mecp2*^{+/-} mice and restored social preference to levels comparable to littermate controls.

We next assessed spatial memory phenotypes using novel object recognition, where *Mecp2*^{+/+} controls showed significantly increased preference for the novel over the familiar object, and vehicle-treated *Mecp2*^{+/-} mice did not discriminate between the two (Fig. 2E). Following VU595 administration, there was no longer a significant difference

between RTT and control test groups, indicating that spatial memory was improved. To determine whether these effects also extended to associative learning, we next progressed mice through a contextual fear assay. Following a mild foot shock, vehicle-treated *Mecp2*^{+/-} mice presented with a significant decrease in time spent freezing compared relative to vehicle-treated controls when re-exposed to the test chamber (Fig. 2F). In contrast, VU595-treated *Mecp2*^{+/-} mice were not distinguishable from controls indicative of a modest improvement in associative memory.

VU595 Improves Respiratory Phenotypes in RTT Mice

Using the decrease in M₁ expression in the brainstem of *Mecp2*^{+/-} mice as rationale, we next assessed VU595's efficacy on respiratory phenotypes using whole-body plethysmography (WBP). Following 30 min of baseline recording,

we administered either vehicle or VU595 and returned the mouse to the recording chamber. After trimming periods of activity from the analysis, drug effects were measured 30 min post-dose (Fig. 3A). Under this paradigm, vehicle-treated *Mecp2*^{+/-} mice exhibited significantly more apneas per 10k breaths than littermate controls, and administration of the M₁ PAM significantly reduced the number of apneas by 49.8% (Fig. 3B). To ensure that this result was

not linked to differences in random × inactivation skewing of the mutant *Mecp2* allele and/or general health differences of *Mecp2*^{+/-} test groups, we compared the number of apneas in individual mice relative to their own pre-drug baseline. During the baseline period, both vehicle and VU595 test groups exhibited a comparable number of apneas (Fig. 3C–D); however, following compound administration, only *Mecp2*^{+/-} mice treated with the M₁

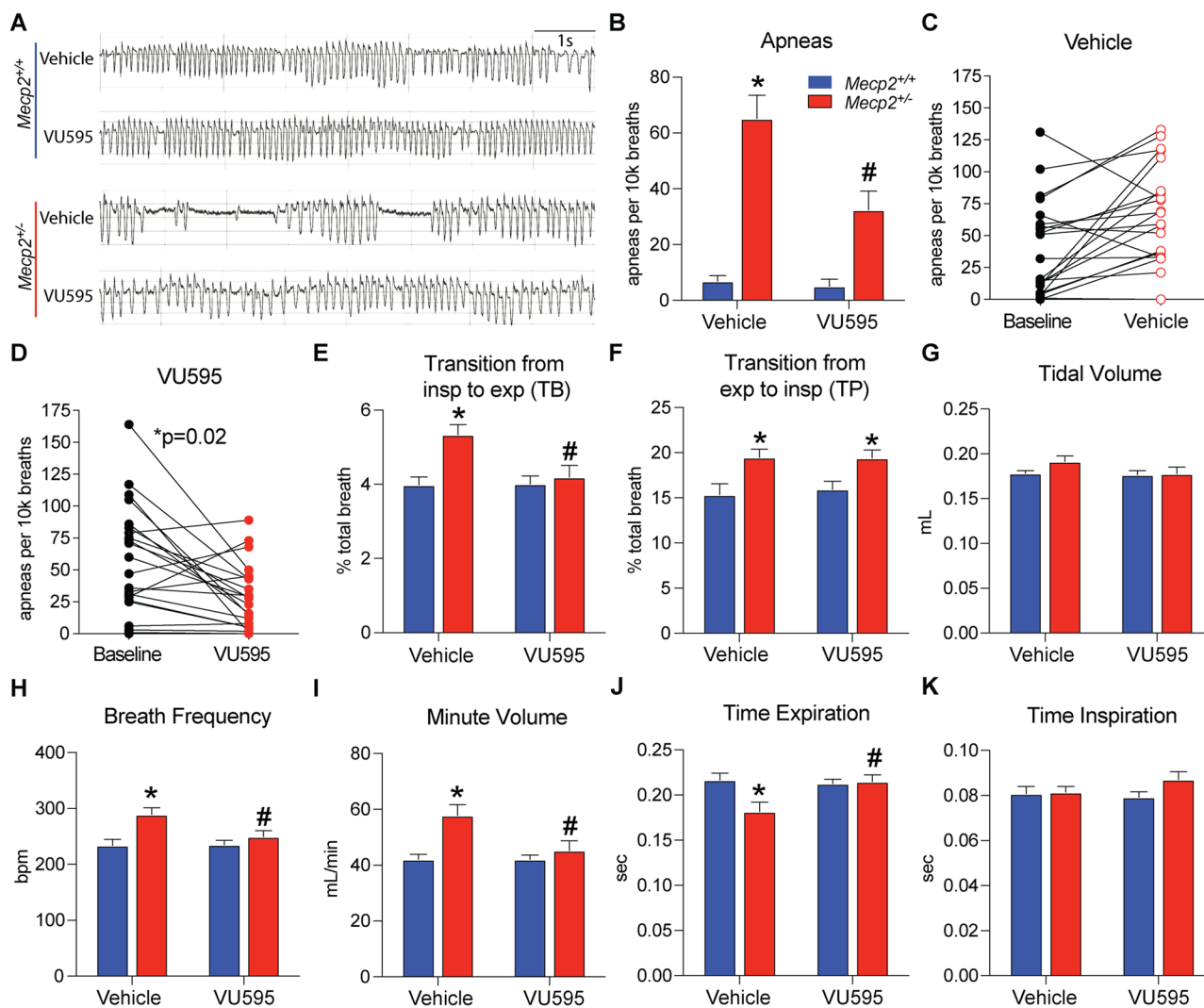


Fig. 3 Administration of VU595 improves apneas by facilitating the transition from inspiration to expiration. Whole-body plethysmography (WBP). Unless noted, statistical comparisons were made relative to vehicle-treated *Mecp2*^{+/-} mice using a two-way ANOVA with Tukey post hoc analysis. *N* = 15 *Mecp2*^{+/-}/treatment group, *N* = 22 *Mecp2*^{+/-}/treatment group. **A** Representative traces of respiratory patterns. **B–D** Apneas were significantly increased in both groups of *Mecp2*^{+/-} mice; however, VU595 treatment significantly reduced the total number of apneas relative to the vehicle-treated group. A comparison relative to the baseline of each mouse shows that both groups of *Mecp2*^{+/-} mice began the experiment with comparable apnea numbers, but that only the VU595-treated group showed significant improvement. **E–F** Vehicle-treated *Mecp2*^{+/-} mice showed a

significant increase in the percentage of the total breath occupied by the pause period between both inspiration and expiration. VU595's efficacy on apneas was associated with a significant reduction in the time between inspiration and expiration, with no effect on the transition from expiration to inspiration. **G** Tidal volume was not impacted by treatment or genotype. **H–I** Breath frequency and minute volume were significantly increased in vehicle-treated *Mecp2*^{+/-} mice and were normalized by VU595 administration. **J–K** Increased breath frequency was associated with a significant decrease in expiratory time in vehicle-treated *Mecp2*^{+/-} mice, which was rescued by VU595 administration. No change in inspiratory time was observed as a function of genotype or treatment. **p* < 0.05 relative to vehicle-treated *Mecp2*^{+/-} mice, #*p* < 0.05 relative to vehicle-treated *Mecp2*^{+/-} mice

PAM showed a significant reduction in apnea numbers, indicative of a *bona fide* compound effect (Fig. 3D).

We next determined the location in the respiratory cycle where VU595 was impacting apneas. We examined the percent of the breath that was spent on the pause period between inspiration and expiration (TB), as well as the percent of time spent paused between expiration and inspiration (TP). In vehicle-treated *Mecp2*^{+/-} mice, both transition points occupied a significantly greater percentage of the breath relative to vehicle-treated *Mecp2*^{+/+} controls (Fig. 3E–F). Conversely, only TB (inspiration to expiration) was normalized by VU595, while the compound did not affect TP (expiration to inspiration). These data suggest that M₁ potentiation decreases apneas in *Mecp2*^{+/-} mice by facilitating the transition between the inspiratory and expiratory phases of the breath cycle.

No effect of drug or genotype was recorded on tidal volume (Fig. 3G); however, we did quantify a significant increase in respiratory frequency in vehicle-treated *Mecp2*^{+/-} mice that was significantly decreased by VU595 administration (Fig. 3H). As a corollary, we also observed a significant increase in the total volume respired per minute (minute volume) in vehicle-treated *Mecp2*^{+/-} mice, which was also normalized by the M₁ PAM (Fig. 3I). To investigate this further, we quantified the amount of time spent in the inspiration phase relative to expiration in each breath. As shown in Fig. 3J–K, the increase in breath frequency and minute volume was associated with a significantly shorter expiratory phase of the breath in vehicle-treated *Mecp2*^{+/-} mice and was normalized with VU595 treatment.

M₁ Potentiation Normalizes Global Gene Expression Patterns

MeCP2 is a highly abundant transcription factor in the brain that regulates gene expression locally in complex with proteins like CREB, as well as globally by linking methylated DNA with the larger chromatin architecture [2]. As a consequence, pathogenic mutations in MeCP2 result in a loosening of chromatin and a broad, but modest disruption of global gene expression patterns. M₁ is a postsynaptic, G_q-coupled receptor whose activation is associated with an increase in intracellular calcium and activation of calcium-dependent transcription factors [32]. To determine whether VU595 normalizes *Mecp2*-disrupted gene expression patterns, we administered either VU595 or vehicle to *Mecp2*^{+/-} and *Mecp2*^{+/+} mice, harvested the brainstem and hippocampus at 30 min post-dose, and performed differential RNA-seq analysis. The brainstem and hippocampus were chosen because they represent regions of the brain associated with apneas and cognition, where M₁ PAM efficacy was observed. A comprehensive list of significantly disrupted

genes and pathways for each brain region is provided in Supplemental Tables 2, 3, 4, 5, 6, 7, 8, and 9.

In the brainstem, vehicle-treated *Mecp2*^{+/-} mice had 2,141 differentially expressed genes (DEGs) relative to vehicle-treated *Mecp2*^{+/+} samples, and 1,384 (64.7%) of those genes were no longer disrupted in mice treated with VU595 (Fig. 4A). Reactome.org (v76) analysis of the normalized genes showed enrichment in pathways associated with assembly and cell surface presentation of NMDARs, among others. We next examined genes that were significantly changed by VU595 treatment in both *Mecp2*^{+/+} and *Mecp2*^{+/-} mice, which identified 119 genes that were affected in both genotypes (Fig. 4B). Pathway analysis of these genes points to an enrichment in FOXO/P21/P53 signaling, which has previously been associated with pathogenic mutations in MeCP2 that disrupt NCoR/HDAC3 binding [33].

In total, 2,727 DEGs were quantified in the hippocampus of vehicle-treated *Mecp2*^{+/-} mice, and 2,294 (84.1%) of those genes were no longer disrupted in *Mecp2*^{+/-} mice treated with VU595 (Fig. 4C). Reactome.org analysis of the normalized genes showed enrichment in pathways associated with the regulation of nonsense-mediated decay and formation of the 40S ribosomal subunit, among many other pathways. The expression of 46 genes exhibited conserved disruption by VU595 in both *Mecp2*^{+/+} and *Mecp2*^{+/-} mice, which demonstrated no significant pathway enrichment (Fig. 4D).

In addition to calcium-dependent gene regulation, M₁ activation impacts the activation of calcium-independent kinases [34], many of which are integral to maintaining proper synaptic transmission. In light of the brainstem RNA-seq and whole-body plethysmography data, one kinase of interest was Gsk3β, which is known to regulate NMDAR trafficking [35] and whose inhibition has been shown to reduce respiratory phenotypes in RTT model mice [36]. To determine whether M₁ potentiation was impacting Gsk3β-signaling, we treated *Mecp2*^{+/+} and *Mecp2*^{+/-} mice with VU595, isolated protein from the brainstem, and performed Western blotting to profile the inhibitory (S9, S21) and activation (Y216/Y279) phosphorylation sites on Gsk3β and its homolog, Gsk3α. Contrary to previous reports [36], we observed no difference in Gsk3β or Gsk3α phosphorylation in *Mecp2*^{+/-} mice relative to vehicle-treated controls at either the inhibitory or activation sites (Fig. 5A–C). Further, neither the inhibitory nor activation sites of Gsk3α were impacted by VU595 administration. Conversely, VU595 treatment significantly increased phosphorylation of the Gsk3β S9 inhibitory site in VU595-treated *Mecp2*^{+/-} mice relative to vehicle-treated *Mecp2*^{+/+} controls, while the activation site was unaffected (Fig. 5D–E). These data suggest that M₁ potentiation promotes inhibition of Gsk3β signaling in the brainstem of RTT model mice, which may contribute to the rescue of respiratory phenotypes independent of a primary deficit in Gsk3β-signaling.

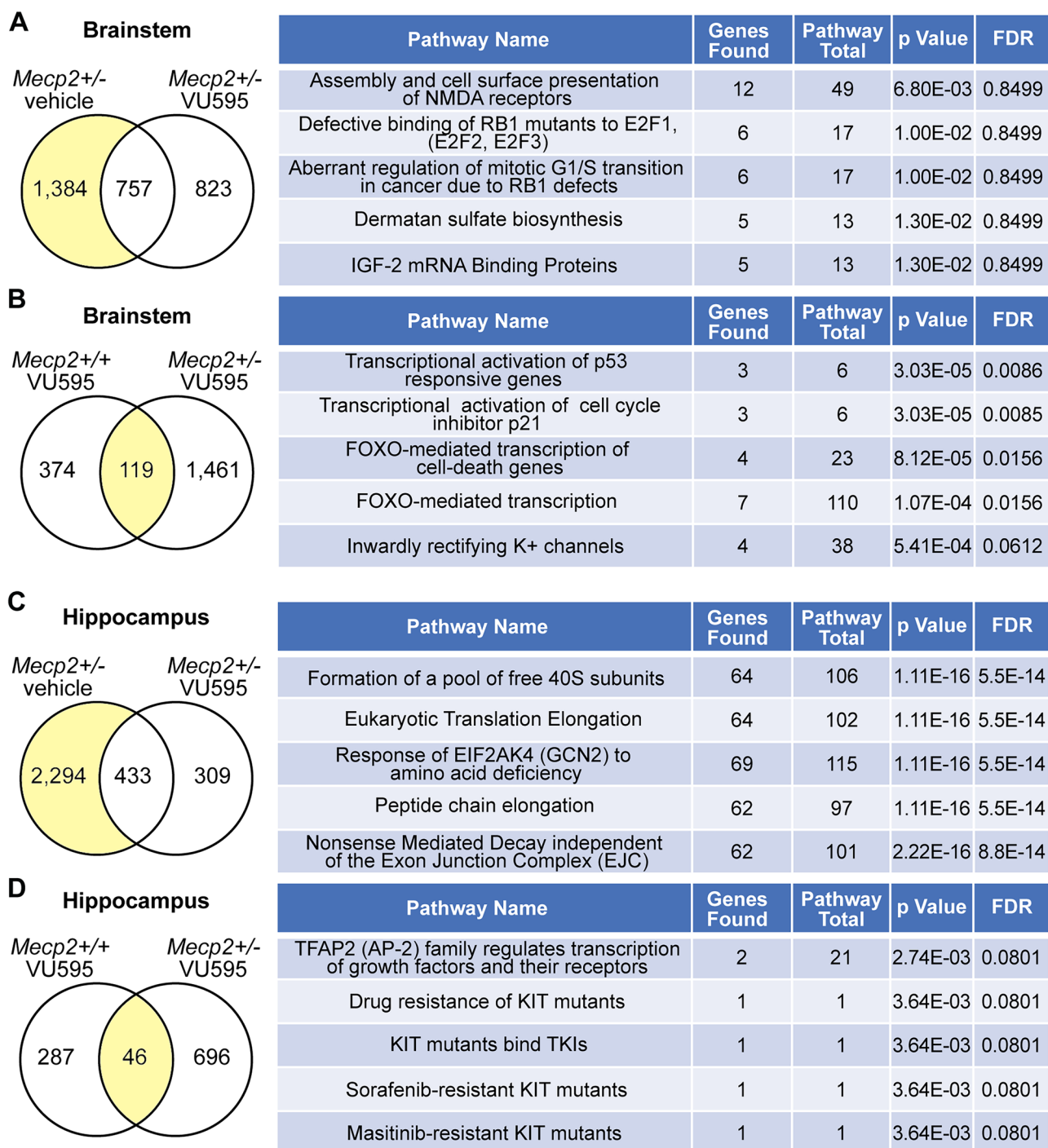


Fig. 4 Global gene expression patterns are normalized by M_1 potentiation. Differential RNA-sequencing relative to vehicle-treated $Mecp2^{+/+}$ control mice followed by reactome pathway enrichment analysis. **A** Brainstem. A total of 2,141 genes were significantly disrupted in vehicle-treated $Mecp2^{+/-}$ mice. Following VU595 treatment, the expression of 1,384 (64.6%) was normalized, while 757 remained disrupted. Right: pathway analysis of rescued genes. **B** Brainstem. Following VU595 administration, the expression of 119 genes was

significantly altered in both $Mecp2^{+/+}$ and $Mecp2^{+/-}$ mice. Right: pathway analysis of conserved genes. **C** Hippocampus. A total of 2,727 genes were significantly disrupted in vehicle-treated $Mecp2^{+/-}$ mice. Following VU595 treatment, the expression of 2,294 (84.1%) was normalized, while 433 remained disrupted. Right: pathway analysis of rescued genes. **D** Hippocampus. Following VU595 administration, the expression of 46 genes was significantly altered in both $Mecp2^{+/+}$ and $Mecp2^{+/-}$ mice. Right: pathway analysis of conserved genes

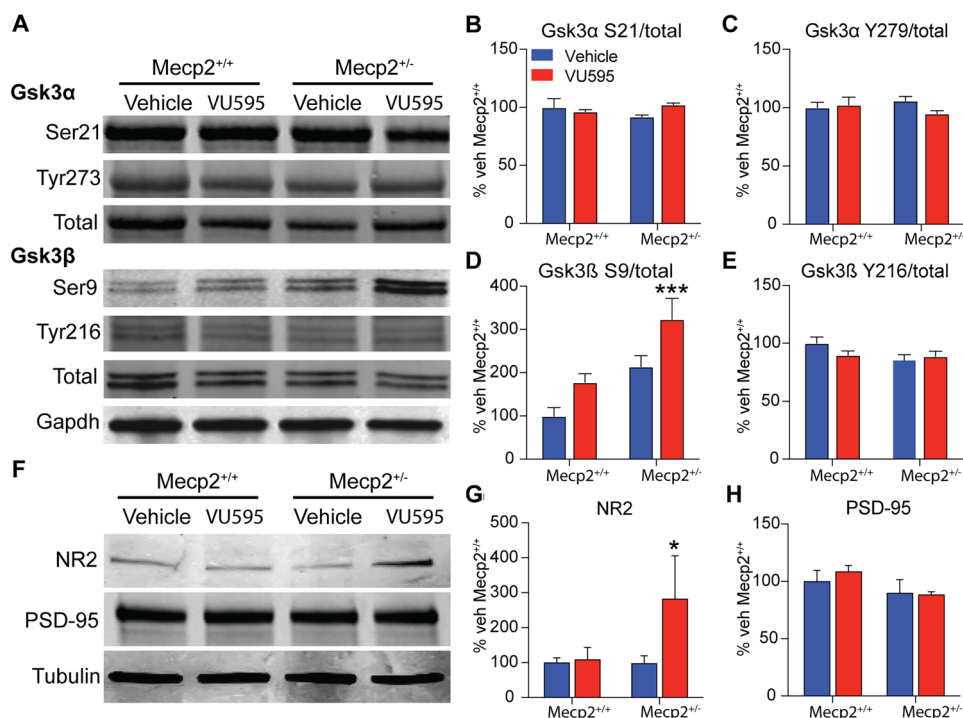


Fig. 5 M₁ potentiation increases both Gsk3β inhibition and synaptic NMDAR levels in the brainstem of *Mecp2*^{+/-} mice. **A** Representative Western blots from the brainstem of *Mecp2*^{+/+} and *Mecp2*^{+/-} mice treated with vehicle or VU595. **B–C** Neither the inhibition (S21) nor the activation (Y279) sites on Gsk3α were significantly impacted by treatment with VU595 as measured by the ratio of phosphorylated (P) to total (T) protein. **D** Administration of VU595 significantly increased the P/T ratio at the S9 inhibitory site of Gsk3β, specifically in the brainstem of *Mecp2*^{+/-} mice, while having no impact in *Mecp2*^{+/+} mice. Two-way ANOVA with Tukey post hoc analysis. **E** The acti-

vation site (Y216) of Gsk3β was not affected in the brainstem by VU595 treatment, regardless of genotype. **F** Representative synaptosome Western blots from the brainstem of *Mecp2*^{+/+} and *Mecp2*^{+/-} mice treated with vehicle or VU595. **G** VU595 significantly increased the presence of NR2a/b containing NMDARs at the synapse of *Mecp2*^{+/-} mice while having no impact on *Mecp2*^{+/+} control mice. Two-way ANOVA with Tukey post hoc analysis. **H** PSD-95 control Western blots confirm that synaptosomes assessed in these experiments contained post-synaptic structures in equivalent amounts across treatments and genotypes. **p* < 0.05, ****p* < 0.001

To determine whether changes in Gsk3β S9 phosphorylation correlated with a change in NMDAR presence at synapses, we isolated PSD95 containing synaptosomes from the brainstem of mice treated with either vehicle or VU595. We then performed Western blotting and probed using a nonselective NR2 subunit antibody. As shown in Fig. 5F–H, there was no difference between vehicle-treated *Mecp2*^{+/+} and *Mecp2*^{+/-} mice; however, VU595 treatment significantly increased the presence of NMDARs at the synapse of *Mecp2*^{+/-} mice relative to controls. While further work is required to establish the functional consequences of increased NMDARs specifically at respiratory nuclei, these data suggest that increased M₁/Gsk3β/NMDAR signaling in the brainstem correlates with the decrease in apneas in RTT model mice induced by the M₁ PAM VU595.

Discussion

Recent clinical development campaigns have shown remarkable progress toward potentially viable Rett syndrome therapeutics [37]. To improve the rigor of our research, we have embraced a reverse-translational approach to target identification. These efforts identified a conserved disruption in mAChRs in RTT autopsy samples [8]. Here, we confirm those findings using a cohort of 40 temporal cortex samples from RTT patients and demonstrate that four of the five mAChRs are significantly decreased in expression. Further, we show that positive allosteric modulation of the M₁ receptor normalizes social preference, associative and spatial memory

deficits, and respiratory phenotypes in *Mecp2*^{+/-} mice, a model with face and construct validity for the clinical disorder [23, 37].

Among our most interesting findings is that *M₁* expression correlated directly with *MeCP2* expression in autopsy samples, such that *M₁* levels are only low when *MeCP2* levels are also low. Given that not all pathogenic mutations impact *MeCP2* gene or protein expression (i.e., missense mutations), these data suggest that decreased *M₁* expression may be enriched in patients with truncating and/or destabilizing mutations [38]. Our sample set precludes testing this hypothesis, as it consists of patients who were clinically diagnosed with RTT, but never genotyped for *MeCP2* mutations. As such, further studies with larger sample sizes are required to substantiate whether a relationship between *MeCP2* mutation and *M₁* expression exists.

The *M₁* receptor has a complicated history as a potential therapeutic target for neurological disorders that is highlighted by the clinical efficacy of the *M₁/M₄*-preferring agonist xanomeline in Alzheimer's disease [17, 18]. The overwhelming majority of subsequent drug discovery efforts were derailed preclinically by the presence of either gastrointestinal or convulsive adverse effects [39]. In recent years, both of these adverse effects have been largely mitigated through selective targeting of the *M₁* receptor with positive allosteric modulators that are void of agonist activity [40–42] and have low cooperativity profiles [43, 44] or by co-dosing xanomeline with a peripherally restricted pan-muscarinic receptor antagonist [19]; however, it bears mentioning in this context since RTT patients are prone to gastrointestinal complications and seizures [45, 46]. We did not observe either phenotype in our studies with *Mecp2*^{+/-} mice, although it remains possible that they might emerge with chronic dosing.

The compound used in our studies, VU595, has previously been shown to exhibit efficacy in correcting abnormal social and spatial memory phenotypes in a chronic phencyclidine (PCP) model of schizophrenia [24], and our data in *Mecp2*^{+/-} mice parallels these findings. Specifically, acute administration of VU595 restored social memory and/or preference in RTT mice without impacting sociability in the three-chamber social interaction assay. Impaired spatial and associated memory phenotypes were also rescued by *M₁* potentiation in the novel object recognition and contextual fear assays, respectively. These results align with *M₁*'s expression pattern, where enrichment is observed at the prefrontal cortical and hippocampal circuits that largely govern these behaviors.

There is a well-established role for mAChRs in the control of breathing [47]; however, this is generally associated with *M₂* and *M₃* receptor expression in the autonomic nervous system and not with *M₁* receptors. Given *M₁*'s limited-expression pattern in the brainstem, it was an unexpected

result that VU595 administration normalized respiratory phenotypes in *Mecp2*^{+/-} mice. While increased breath rate has previously been reported in *Mecp2*^{+/-} mice [48], here we link this finding in vehicle-treated mice with a decrease in expiratory time. Equally as important as the impact of VU595 on breath rate is its capacity to decrease apneas, which our data link to facilitation of the transition from inspiration to expiration. This finding agrees with in situ physiology data showing that increased post-inspiratory duration is associated with hyperexcitation of expiratory inputs originating in the Kölliker-Fuse nucleus in *Mecp2*^{-/-} mice [49]. In agreement with these data, glutamate microinjection at these inputs can evoke apneas in ex vivo preparations from the same model [48, 50]. Accordingly, our data may suggest that *M₁* potentiation may decrease apneas by tempering hyperexcitation in the Kölliker-Fuse nucleus, although this will need to be tested experimentally.

Our RNA-sequencing experiments established that one of the top pathways that was rescued in the brainstem of VU595-treated *Mecp2*^{+/-} animals involves the assembly and trafficking of NMDARs, and follow-up studies implicate Gsk3 β inhibition in mediating the observed efficacy. NMDA-signaling has a well-developed history in RTT research, where both deletion of the NR2A subunit [28] and administration of the NMDAR antagonist ketamine rescue multiple aspects of RTT pathophysiology in mice [51–53]. Previous studies have also shown that Gsk3 β inhibition rescues multiple symptom domains, including respiration [36], and is known to regulate NMDAR activity and trafficking, in part, via activation of phosphatidylinositol 4 kinase type II α (PI4KII α) [35]. NMDAR activation has been shown to dephosphorylate the S9 inhibitory site of Gsk3 β [54], thereby providing a mechanistic point of convergence for ketamine, VU595 (*M₁* PAM), and SB216763 (Gsk3 β inhibitor) to act on apneas in the brainstem of RTT model mice. One important aspect of our data quantifying Gsk3 β inhibition is that it was not significantly affected in the brainstem of vehicle-treated *Mecp2*^{+/-} mice, and trended towards an increased baseline, as has previously been reported in other brain regions (36). This suggests that insufficient Gsk3 β inhibition is likely not the driver of respiratory phenotypes. When analyzed in concert with the SB216763 data, one potential unifying explanation is that Gsk3 β inhibition is a compensatory mechanism that cannot reach the required levels to maintain proper respiratory function in the absence of *Mecp2* due to decreased *M₁*-expression and signaling. If true, it would suggest that VU595 and SB216763 function by enhancing an existing neuroprotective mechanism to regulate synaptic NMDAR levels; however, further work is required to determine if this is a *bona fide* mechanism of action.

In summary, we describe the use of a large cohort of temporal cortex autopsy samples from RTT patients to establish the rationale for the *M₁* receptor as a potential therapeutic

target. Drug discovery campaigns for positive modulators of mAChRs have made significant advancements in recent years, such that compounds with favorable drug-like properties now exist. Using the M₁ PAM tool compound VU595, we observed efficacy in social, cognitive, and respiratory symptom domains in *Mecp2*^{+/-} mice. Phenotypic improvement was correlated with both normalization of gene expression and increased inhibition of Gsk3 β . Together, these data advocate for continued development and optimization of M₁ PAMs for RTT, as well as for related autism-associated disorders with overlapping pathologies.

Supplementary Information The online version contains supplementary material available at <https://doi.org/10.1007/s13311-022-01254-3>.

Acknowledgements The authors acknowledge and thank P. Jeffrey Conn (PJC) for financial and conceptual contributions to the proposed work. Harvard Brain Tissue Resource Center is supported by Public Health Service contract HHSN-271-2013-00030, and the University of Maryland Brain Bank is a tissue repository of the National Institutes of Health (NIH) NeuroBioBank. RGG received support from a Young Investigator Award from the Brain and Behavior Research Foundation, K01MH112983, and R01NS112171. NMF and SADV were supported by training grant NIH T32 GM007628-36, F31MH119699, F31MH113259, and the Vanderbilt Program in Molecular Medicine (VPM). The authors would also like to acknowledge 3503 from IRSF (CMN) and 3903 from IRSF (RGG, CMN).

Declarations

Competing Interests CWL and CMN receive research support from Acadia Pharmaceuticals and Boehringer Ingelheim, and CWL also received support from Ono Pharmaceutical. CWL and CMN are inventors on multiple patents for allosteric modulators of muscarinic acetylcholine receptors. All other authors declare no potential conflicts of interest.

Open Access This article is licensed under a Creative Commons Attribution 4.0 International License, which permits use, sharing, adaptation, distribution and reproduction in any medium or format, as long as you give appropriate credit to the original author(s) and the source, provide a link to the Creative Commons licence, and indicate if changes were made. The images or other third party material in this article are included in the article's Creative Commons licence, unless indicated otherwise in a credit line to the material. If material is not included in the article's Creative Commons licence and your intended use is not permitted by statutory regulation or exceeds the permitted use, you will need to obtain permission directly from the copyright holder. To view a copy of this licence, visit <http://creativecommons.org/licenses/by/4.0/>.

References

- Amir RE, Van den Veyver IB, Wan M, Tran CQ, Francke U, Zoghbi HY. Rett syndrome is caused by mutations in X-linked MECP2, encoding methyl-CpG-binding protein 2. *Nat Genet.* 1999;23(2):185–8.
- Chahrouh M, Jung SY, Shaw C, Zhou X, Wong ST, Qin J, et al. MeCP2, a key contributor to neurological disease, activates and represses transcription. *Science.* 2008;320(5880):1224–9.
- Lyst MJ, Ekiert R, Ebert DH, Merusi C, Nowak J, Selfridge J, et al. Rett syndrome mutations abolish the interaction of MeCP2 with the NCoR/SMRT co-repressor. *Nat Neurosci.* 2013;16(7):898–902.
- Shah RR, Bird AP. MeCP2 mutations: progress towards understanding and treating Rett syndrome. *Genome Med.* 2017;9(1):17.
- Percy AK, Lane JB. Rett syndrome: clinical and molecular update. *Curr Opin Pediatr.* 2004;16(6):670–7.
- Percy AK. Rett syndrome. *Curr Opin Neurol.* 1995;8(2):156–60.
- Gamo NJ, Birknow MR, Sullivan D, Kondo MA, Horiuchi Y, Sakurai T, et al. Valley of death: A proposal to build a “translational bridge” for the next generation. *Neurosci Res.* 2017;115:1–4.
- Gogliotti RG, Fisher NM, Stansley BJ, Jones CK, Lindsley CW, Conn PJ, et al. Total RNA sequencing of Rett syndrome autopsy samples identifies the M4 muscarinic receptor as a novel therapeutic target. *J Pharmacol Exp Ther.* 2018;365(2):291–300.
- Gogliotti RG, Senter RK, Fisher NM, Adams J, Zamorano R, Walker AG, et al. mGlu7 potentiation rescues cognitive, social, and respiratory phenotypes in a mouse model of Rett syndrome. *Sci Transl Med.* 2017;9(403).
- Wenk GL, Mobley SL. Choline acetyltransferase activity and vesicular binding in Rett syndrome and in rats with nucleus basalis lesions. *Neuroscience.* 1996;73(1):79–84.
- Johnston MV, Hohmann C, Blue ME. Neurobiology of Rett syndrome. *Neuropediatrics.* 1995;26(2):119–22.
- Murasawa H, Kobayashi H, Imai J, Nagase T, Soumiya H, Fukumitsu H. Substantial acetylcholine reduction in multiple brain regions of *Mecp2*-deficient female rats and associated behavioral abnormalities. *PLoS ONE.* 2021;16(10):e0258830.
- Ballinger EC, Schaaf CP, Patel AJ, de Maio A, Tao H, Talmage DA, et al. *Mecp2* deletion from cholinergic neurons selectively impairs recognition memory and disrupts cholinergic modulation of the perirhinal cortex. *eNeuro.* 2019;6(6).
- Zhang S, Johnson CM, Cui N, Xing H, Zhong W, Wu Y, et al. An optogenetic mouse model of rett syndrome targeting on catecholaminergic neurons. *J Neurosci Res.* 2016;94(10):896–906.
- Zhang Y, Zhu Y, Cao SX, Sun P, Yang JM, Xia YF, et al. MeCP2 in cholinergic interneurons of nucleus accumbens regulates fear learning. *Elife.* 2020;9.
- Nag N, Berger-Sweeney JE. Postnatal dietary choline supplementation alters behavior in a mouse model of Rett syndrome. *Neurobiol Dis.* 2007;26(2):473–80.
- Bodick NC, Offen WW, Levey AI, Cutler NR, Gauthier SG, Satlin A, et al. Effects of xanomeline, a selective muscarinic receptor agonist, on cognitive function and behavioral symptoms in Alzheimer disease. *Arch Neurol.* 1997;54(4):465–73.
- Rusted JM, Warburton DM. The effects of scopolamine on working memory in healthy young volunteers. *Psychopharmacology.* 1988;96(2):145–52.
- Brannan SK, Sawchak S, Miller AC, Lieberman JA, Paul SM, Breier A. Muscarinic cholinergic receptor agonist and peripheral antagonist for schizophrenia. *N Engl J Med.* 2021;384(8):717–26.
- Garg SK, Lioy DT, Cheval H, McGann JC, Bissonnette JM, Murtha MJ, et al. Systemic delivery of MeCP2 rescues behavioral and cellular deficits in female mouse models of Rett syndrome. *J Neurosci.* 2013;33(34):13612–20.
- Samaco RC, McGraw CM, Ward CS, Sun Y, Neul JL, Zoghbi HY. Female *Mecp2*(+/-) mice display robust behavioral deficits on two different genetic backgrounds providing a framework for pre-clinical studies. *Hum Mol Genet.* 2013;22(1):96–109.
- Stearns NA, Schaevitz LR, Bowling H, Nag N, Berger UV, Berger-Sweeney J. Behavioral and anatomical abnormalities in *Mecp2* mutant mice: a model for Rett syndrome. *Neuroscience.* 2007;146(3):907–21.

23. Gogliotti RG, Niswender CM. A coordinated attack: Rett syndrome therapeutic development. *Trends Pharmacol Sci.* 2019;40(4):233–6.
24. Ghoshal A, Rook JM, Dickerson JW, Roop GN, Morrison RD, Jalan-Sakrikar N, et al. Potentiation of M1 muscarinic receptor reverses plasticity deficits and negative and cognitive symptoms in a schizophrenia mouse model. *Neuropsychopharmacology.* 2016;41(2):598–610.
25. Leger M, Quiedeville A, Bouet V, Haelewyn B, Boulouard M, Schumann-Bard P, et al. Object recognition test in mice. *Nat Protoc.* 2013;8(12):2531–7.
26. Jositsch G, Papadakis T, Haberberger RV, Wolff M, Wess J, Kummer W. Suitability of muscarinic acetylcholine receptor antibodies for immunohistochemistry evaluated on tissue sections of receptor gene-deficient mice. *Naunyn Schmiedebergs Arch Pharmacol.* 2009;379(4):389–95.
27. Degano AL, Park MJ, Penati J, Li Q, Ronnett GV. MeCP2 is required for activity-dependent refinement of olfactory circuits. *Mol Cell Neurosci.* 2014;59:63–75.
28. Durand S, Patrizi A, Quast KB, Hachigian L, Pavlyuk R, Saxena A, et al. NMDA receptor regulation prevents regression of visual cortical function in the absence of MeCP2. *Neuron.* 2012;76(6):1078–90.
29. Krishnan K, Wang BS, Lu J, Wang L, Maffei A, Cang J, et al. MeCP2 regulates the timing of critical period plasticity that shapes functional connectivity in primary visual cortex. *Proc Natl Acad Sci U S A.* 2015;112(34):E4782–91.
30. Lee LJ, Tsytsarev V, Erzurumlu RS. Structural and functional differences in the barrel cortex of MeCP2 null mice. *J Comp Neurol.* 2017;525(18):3951–61.
31. Orefice LL, Zimmerman AL, Chirila AM, Sleboda SJ, Head JP, Ginty DD. Peripheral mechanosensory neuron dysfunction underlies tactile and behavioral deficits in mouse models of ASDs. *Cell.* 2016;166(2):299–313.
32. Wess J. Molecular basis of muscarinic acetylcholine receptor function. *Trends Pharmacol Sci.* 1993;14(8):308–13.
33. Nott A, Cheng J, Gao F, Lin YT, Gjonjeska E, Ko T, et al. Histone deacetylase 3 associates with MeCP2 to regulate FOXO and social behavior. *Nat Neurosci.* 2016;19(11):1497–505.
34. Lanzafame AA, Christopoulos A, Mitchelson F. Cellular signaling mechanisms for muscarinic acetylcholine receptors. *Recept Channels.* 2003;9(4):241–60.
35. Amici M, Lee Y, Pope RJP, Bradley CA, Cole A, Collingridge GL. GSK-3beta regulates the synaptic expression of NMDA receptors via phosphorylation of phosphatidylinositol 4 kinase type IIalpha. *Eur J Neurosci.* 2021;54(8):6815–25.
36. Jorge-Torres OC, Szczesna K, Roa L, Casal C, Gonzalez-Somermeyer L, Soler M, et al. Inhibition of Gsk3b reduces Nfkb1 signaling and rescues synaptic activity to improve the Rett syndrome phenotype in MeCP2-knockout mice. *Cell Rep.* 2018;23(6):1665–77.
37. Katz DM, Berger-Sweeney JE, Eubanks JH, Justice MJ, Neul JL, Pozzo-Miller L, et al. Preclinical research in Rett syndrome: setting the foundation for translational success. *Dis Model Mech.* 2012;5(6):733–45.
38. Tillotson R, Bird A. The molecular basis of MeCP2 function in the brain. *J Mol Biol.* 2019.
39. Voss T, Li J, Cummings J, Farlow M, Assaid C, Froman S, et al. Randomized, controlled, proof-of-concept trial of MK-7622 in Alzheimer's disease. *Alzheimers Dement (N Y).* 2018;4:173–81.
40. Moran SP, Cho HP, Maksymetz J, Remke DH, Hanson RM, Niswender CM, et al. PF-06827443 displays robust allosteric agonist and positive allosteric modulator activity in high receptor reserve and native systems. *ACS Chem Neurosci.* 2018;9(9):2218–24.
41. Moran SP, Dickerson JW, Cho HP, Xiang Z, Maksymetz J, Remke DH, et al. M1-positive allosteric modulators lacking agonist activity provide the optimal profile for enhancing cognition. *Neuropsychopharmacology.* 2018;43(8):1763–71.
42. Rook JM, Bertron JL, Cho HP, Garcia-Barrantes PM, Moran SP, Maksymetz JT, et al. A novel M1 PAM VU0486846 exerts efficacy in cognition models without displaying agonist activity or cholinergic toxicity. *ACS Chem Neurosci.* 2018;9(9):2274–85.
43. Mandai T, Sako Y, Kurimoto E, Shimizu Y, Nakamura M, Fushimi M, et al. T-495, a novel low cooperative M1 receptor positive allosteric modulator, improves memory deficits associated with cholinergic dysfunction and is characterized by low gastrointestinal side effect risk. *Pharmacol Res Perspect.* 2020;8(1):e00560.
44. Sako Y, Kurimoto E, Mandai T, Suzuki A, Tanaka M, Suzuki M, et al. TAK-071, a novel M1 positive allosteric modulator with low cooperativity, improves cognitive function in rodents with few cholinergic side effects. *Neuropsychopharmacology.* 2019;44(5):950–60.
45. Fu C, Armstrong D, Marsh E, Lieberman D, Motil K, Witt R, et al. Multisystem comorbidities in classic Rett syndrome: a scoping review. *BMJ Paediatr Open.* 2020;4(1):e000731.
46. Guerrini R, Parrini E. Epilepsy in Rett syndrome, and CDKL5- and FOXP1-gene-related encephalopathies. *Epilepsia.* 2012;53(12):2067–78.
47. Douglas CL, Demarco GJ, Baghdoyan HA, Lydic R. Pontine and basal forebrain cholinergic interaction: implications for sleep and breathing. *Respir Physiol Neurobiol.* 2004;143(2–3):251–62.
48. Ward CS, Huang TW, Herrera JA, Samaco RC, McGraw CM, Parra DE, et al. Loss of MeCP2 function across several neuronal populations impairs breathing response to acute hypoxia. *Front Neurol.* 2020;11:593554.
49. Stettner GM, Huppke P, Brendel C, Richter DW, Gartner J, Dutschmann M. Breathing dysfunctions associated with impaired control of postinspiratory activity in MeCP2-/- knockout mice. *J Physiol.* 2007;579(Pt 3):863–76.
50. Weese-Mayer DE, Lieske SP, Boothby CM, Kenny AS, Bennett HL, Silvestri JM, et al. Autonomic nervous system dysregulation: breathing and heart rate perturbation during wakefulness in young girls with Rett syndrome. *Pediatr Res.* 2006;60(4):443–9.
51. Patrizi A, Picard N, Simon AJ, Gunner G, Centofante E, Andrews NA, et al. Chronic administration of the N-methyl-D-aspartate receptor antagonist ketamine improves Rett syndrome phenotype. *Biol Psychiatry.* 2016;79(9):755–64.
52. Kron M, Howell CJ, Adams IT, Ransbottom M, Christian D, Ogier M, et al. Brain activity mapping in MeCP2 mutant mice reveals functional deficits in forebrain circuits, including key nodes in the default mode network, that are reversed with ketamine treatment. *J Neurosci.* 2012;32(40):13860–72.
53. Katz DM, Menniti FS, Mather RJ. N-methyl-D-aspartate receptors, ketamine, and Rett syndrome: something special on the road to treatments?. *Biol Psychiatry.* 2016;79(9):710–2.
54. Sztatmari E, Habas A, Yang P, Zheng JJ, Hagg T, Hetman M. A positive feedback loop between glycogen synthase kinase 3beta and protein phosphatase 1 after stimulation of NR2B NMDA receptors in forebrain neurons. *J Biol Chem.* 2005;280(45):37526–35.

Publisher's Note Springer Nature remains neutral with regard to jurisdictional claims in published maps and institutional affiliations.